magnetochemistry

MDPI

Article

Magnetic CS/PVA Composite Materials for the Removal of Pb(II) from Aqueous Solutions

Xuemei Lin [1,2], Wei Lin [1] and Yunhong Li [1,*]

[1] Laboratory Management Center, Hebei Minzu Normal University, Chengde 067000, China; lxm@hbun.edu.cn (X.L.); linweil@hbun.edu.cn.com (W.L.)
[2] Hebei Province Chengde Center for Technological Innovation in Clean Energy and Ecological Protection, Chengde 067000, China
* Correspondence: lyh@hbun.edu.cn; Tel.: +86-15731469321

Abstract

In this article, Fe_3O_4 magnetic particles were prepared via the coprecipitation method, and composite materials (PMCTS) were prepared via a crosslinking reaction of chitosan, polyvinyl alcohol and magnetic particles with glutaraldehydel. The composition, structure, morphology, and magnetic properties of the composite materials were characterized. The effects of the materials input, initial concentration of Pb(II), adsorption time, and temperature on the adsorption performance of PMCTS were further investigated, and the recovery rate of the materials was analyzed. The experiment shows that when the Pb(II) content in water is 30 mg/L, 0.5 g PMCTS are added to the adsorption system, the reaction time is 70 min at 45 °C, and pH = 7, the Pb(II) removal rate can reach 98.9%, and the recovery rate can reach 91.6%. Therefore, PMCTS are fast and effective in adsorbing Pb(II) in water.

Keywords: chitosan; polyvinyl alcohol; composite materials; adsorption

1. Introduction

Heavy metal pollutants originally existed in the natural environment. However, due to human activities, the concentration of heavy metals in the environment has greatly increased, and they have entered the water body through surface runoff, atmospheric deposition and other diffusion methods [1]. Due to the biomagnification of heavy metals, they can directly or indirectly affect various organisms. Many heavy metal ions, such as lead, cadmium, arsenic, manganese and mercury, have toxic and carcinogenic effects. Even at very low concentrations, they can cause multiple organ damage and even cause neurodegenerative diseases such as Alzheimer's disease and Parkinson's disease [2]. Heavy metal ions can also affect aquatic organisms (phytoplankton, zooplankton and fish) and accumulate in multiple organs, leading to oxidative damage, endocrine disorders and immune system inhibition, thereby affecting the survival and growth of aquatic organisms [3]. Lead is one of the most toxic heavy metals, which is extremely harmful to human health even at low concentrations. When lead accumulates in the human body, it can affect organelles in cells, such as mitochondria, nuclei, lysosomes and cell membranes, causing serious damage to nerves and kidneys. In addition, heavy metals interact with DNA and nucleoproteins, causing DNA damage, leading to cell apoptosis or a class of pollutants [4]. Research on the treatment methods and technologies for Pb(II)-containing wastewater has attracted great attention. At present, the chemical precipitation method, membrane separation method and adsorption method are the main methods of removing Pb(II) from wastewater, which

Check for updates

Academic Editor: Carlos J. Gómez García

Received: 31 March 2026
Revised: 26 May 2026
Accepted: 26 May 2026
Published: 1 June 2026

Copyright: © 2026 by the authors. Licensee MDPI, Basel, Switzerland. This article is an open access article distributed under the terms and conditions of the Creative Commons Attribution (CC BY) license.

each have their own advantages and disadvantages. Among them, the adsorption method has become the most economical and effective treatment method because of its easy access to adsorption materials, low cost, strong stability, simple operation and high efficiency. Finding cheap and efficient adsorption materials is of key concern.

Chitosan (CS), as a degradable natural polymer, is widely used in chemical industries, agriculture, water treatment and metal recovery due to its advantages of non-toxicity and low cost. Because of the active hydroxyl (-OH) and amino (-NH_2) groups on the chitosan molecule, it can bind to many metal ions and organic compounds, and it can also be used to prepare composite materials with other materials, for which it is widely used in water treatment technology research [5–10]. Jin et al. [11] studied the influence mechanism of solution pH value on the adsorption of Pb(II) in wastewater by cross-linked chitosan/polyvinyl alcohol (CS/PVA) microspheres through batch adsorption experiments, Fourier transform infrared spectroscopy and X-ray photoelectron spectroscopy. The adsorption mechanism of Pb(II) in wastewater by cross-linked chitosan/polyvinyl alcohol microspheres at different pH values provides methodological guidance for the study of the adsorption of heavy metal ions in wastewater by chitosan/polyvinyl alcohol microspheres. Kumar et al. [12] prepared cross-linked chitosan/polyvinyl alcohol microspheres with chemical stability in acidic media, which can effectively recover Cd(II) in wastewater, providing a theoretical basis for the application of cross-linked chitosan/polyvinyl alcohol microspheres to remove heavy metal ions in wastewater. Laus et al. [13] studied the adsorption capacity of heavy metal ions Cu(II), Pb(II) and Cd(II) in wastewater by crosslinking chitosan with epichlorohydrin and triphosphate through covalent bonds and ionic bonds. Liu et al. [14] studied the adsorption process of heavy metal ions Cu(II), Pb(II), Cd(II), Zn(II) and Ni(II) in wastewater using nanofibrillated chitosan as a chelating agent. It was found that the adsorption process conformed to the Langmuir isotherm and the pseudo-second-order kinetic model. Kandile et al. [15] prepared a novel chitosan hydrogel with 1,3-(dioxoisoindoline-2-amino) as the modified group for the first time and applied it to adsorb heavy metal ions Co(II), Hg(II), Cu(II), Zn(II) and Pb(II) in wastewater. The results showed that it only had good adsorption efficiency for Co(II) and Hg(II). Shen et al. [16] synthesized HTC-chitosan via the hydrothermal carbonization method, and its adsorption efficiency for Cr(VI) in wastewater exceeded 92%. Khawar et al. [17] studied the adsorption properties of Pb(II) in wastewater by adsorbents synthesized from chitosan, diammonium phosphate and ethylenediaminetetraacetic acid. Goudarzi, T. et al. [18] prepared three kinds of organic–inorganic nanocomposites based on magnetic chitosan (such as CS-$MnFe_2O_4$, CS-$MnFe_2O_4$-CoS and CS-$MnFe_2O_4$-CoS-MWCNTs) to explore their ability to adsorb mercury ions from aqueous solutions. Wang, W.R. et al. [19] prepared two novel, highly selective, acid-resistant and reusable functionalized magnetic chitosan composites (FOS@C-DTPA and FOS@C-PBTCA). Highly efficient and selective uranium extraction was achieved by using an anion-assisted synergistic mechanism.

In this paper, chitosan, magnetic Fe_3O_4 and polyvinyl alcohol were used as raw materials to prepare PMCTS under the crosslinking effect of glutaraldehyde. The adsorption performance of composite materials on Pb(II) in wastewater was investigated, and the main factors of adsorption were analyzed. At the same time, the recovery of PMCTS was investigated in order to provide a theoretical basis for the treatment of wastewater containing Pb(II) with chitosan composite materials.

2. Materials and Methods

2.1. Chemicals

Chitosan (CS, degree of deacetylation 90%), polyvinyl alcohol (PVA, 2000), absolute ethanol, $FeCl_3$, $FeCl_2 \cdot 6H_2O$, Span-80, liquid paraffin, acetone, 50% glutaraldehyde,

glacial acetic acid, sodium hydroxide, etc., are all analytically pure; bivalent lead standard, 1 mg/mL.

All solvents and reagents were purchased from China Tianjin Kermel Chemical Reagent Co., Ltd. (Tianjin, China).

2.2. Synthesis of CS/PVA Magnetic Composite Materials

Magnetic Fe_3O_4 nanoparticles were prepared via the co-precipitation method. A certain amount of $FeCl_3$ and $FeCl_2 \bullet 6H_2O$ solution was dissolved in a ratio of 1:1.75 to obtain a mixed solution. In the N_2 atmosphere, the NaOH solution was slowly added to the mixed system, adjusted to pH = 10, quickly stirred, and crystallized in a constant-temperature water bath at 60 °C for 1 h. The mixed system gradually changed from orange red to black, and then stirring was continued for 15 min. The obtained product was centrifuged and precipitated, washed repeatedly with deionized water and anhydrous ethanol until neutral, and dried at 80 °C for 12 h to obtain magnetic Fe_3O_4 nanoparticles. A total of 1.5 g chitosan was dissolved in 100 mL 3% acetic acid solution and stirred at 50 °C until dissolved. We took a 50 mL chitosan solution and added 0.1 g Fe_3O_4 nanoparticles. The solution underwent ultrasonic dispersion for 30 min, and we obtained a uniform solution for later use. A total of 1.5 g polyvinyl alcohol was added into 50 mL deionized water. The solution was first swollen in cold water for 30 min, then slowly heated to 90 °C, and dissolved and dispersed for 1 h under constant-temperature water bath stirring. The above two solutions were mixed evenly to obtain a mixture.

The mixture was added drop by drop to a three-neck flask containing 80 mL of liquid paraffin and 5 mL of Span-80 with a disposable syringe, and quickly stirred for 1 h at room temperature. We added 10% glutaraldehyde, 8 mL. The mixture was heated to 40 °C in a rapid stirring reaction for 1 h. A total of 1.0 M NaOH solution was added to maintain the pH value of the system at 9–10. After the water bath temperature was increased to 70 °C, the stirring reaction was continued for 2 h. The obtained product was fully washed with petroleum ether, acetone and deionized water. PMCTS were obtained by drying at 50 °C, grinding, and passing through an 80 mesh sieve, as shown in Figure 1.

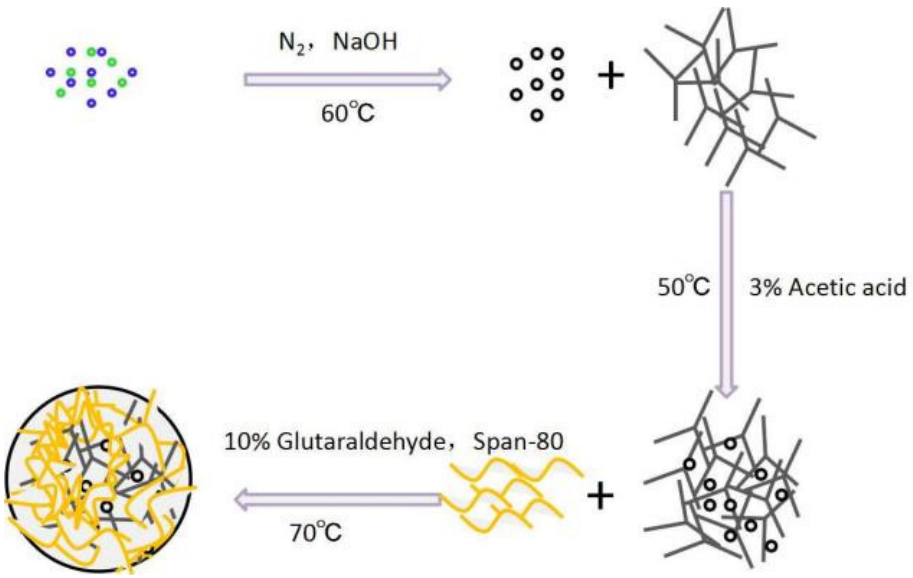


Figure 1. Preparation flow chart of PMCTS.

2.3. Characterization of PMCTS

The PMCTS were qualitatively analyzed by infrared spectroscopy (FTIR-8300, SHIMATZU, Kyoto, Japan) in the wavelength range of 400–4000 cm^{-1}. The morphology and

particle size distribution of PMCTS were analyzed by an X-ray diffractometer (XRD, SmartLab, Rigaku, Tokyo, Japan) and scanning electron microscope (SEM, JSM-7610FPlus, JEOL, Tokyo, Japan). The magnetic properties of the materials were characterized by a vibrating sample magnetometer (VSM, Lake Shore-7404, Westerville, OH, USA).

2.4. Absorption Experiment

A certain amount of Pb(II) standard solution was placed in a 50 mL stoppered colorimetric tube, and deionized water was added to the scale line. A certain amount of PMCTS was added and reacted in a 150 r/min constant-temperature shaker. After the reaction, the concentration of Pb(II) in the solution was determined by an ultraviolet spectrophotometer (UV, 754N, YOKE, Shanghai, China).

(1) The standard solution containing Pb(II) was prepared, and the color reagent was added. The absorbance was measured at 540 nm, and the standard curve was drawn.

(2) According to the single factor variable method, the effects of the dosage of PMCTS, the initial concentration of Pb(II), the temperature of the water bath, the adsorption reaction time, and the pH on the adsorption effect of Pb(II) were investigated.

2.5. Analysis of Recovery Rate of PMCTS

Using the magnetic characteristics of the composite materials, the recovery experiment of the adsorbent materials was carried out with a magnet. First, 1 g of PMCTS was put into simulated wastewater containing Pb(II). After 70 min of reaction adsorption, magnetic adsorption was carried out to remove the liquid and recover the adsorbent. The adsorbent was dried at 75 °C for 1 h, and the recovery rate was calculated by weighing.

2.6. Adsorption Mechanism

2.6.1. Adsorption Kinetics

The adsorption kinetics of Pb(II) on PMCTS was further studied. The pseudo-first-order kinetic model and the pseudo-second-order kinetic model were used to fit the kinetic experimental data. We took 100 mL of Pb(II) solution (50 mg/L, pH = 7), added 50 mg PMCTS, and shook it at 45 °C. The adsorption time was 5, 10, 20, 30, 40, 50, 60, 70, and 80 respectively, and the absorbance of the supernatant was measured. The adsorption amounts at different times were calculated, and the $\ln(Q_e - Q_t)$ versus t and t/Q_t versus t were plotted, respectively. The fitting parameters of the adsorption kinetic equation were obtained via the linear fitting curve of the pseudo-first-order kinetic equation and the pseudo-second-order kinetic equation. The rate-controlling step in the adsorption process was judged by the degree of fitting. The pseudo-first-order kinetic equation can be seen in Formula (1), and the pseudo-second-order kinetic equation can be seen in Formula (2).

$$\ln(Q_e - Q_t) = \ln Q_e - K_1 t \quad (1)$$

$$\frac{t}{Q_t} = \frac{1}{K_2 Q_e^2} + \frac{t}{Q_e} \quad (2)$$

Q_e is the amount of Pb(II) adsorbed by the adsorbent at equilibrium, (mg/g); Q_t is the amount of residual Pb(II) in the solution at time t, (mg/g); K_1 is the equilibrium constant of the first-order adsorption rate; and K_2 is the equilibrium constant of the second-order adsorption rate.

2.6.2. Adsorption Isotherm

We took 100 mL Pb(II) solution (pH = 7) with concentrations of 25, 40, 60, 80, 100, 120 and 150 mg/L, added 50 mg PMCTS, and shook it in a constant-temperature shaker at

45 °C for 80 min. The absorbance of the supernatant was measured, and the adsorption amount was calculated.

In order to further study the mechanism of Pb(II) adsorption by modified materials, the Langmuir equation and Freundlich equation were used to linearly fit the obtained experimental data, as shown in Equations (3) and (4). The Langmuir and Freundlich adsorption isotherms and fitting parameters of the adsorbent at 45 °C were obtained by plotting c_e/Q_e to c_e and $\ln Q_e$ to $\ln c_e$, respectively.

$$\frac{C_e}{Q_e} = \frac{1}{Q}C_e + \frac{1}{Q_b} \tag{3}$$

$$\ln Q_e = \ln K_F + b_F \ln C_e \tag{4}$$

Q is the maximum monolayer adsorption capacity of the adsorbent, mg/g; b is the adsorption equilibrium constant; Q_e is the adsorption capacity at equilibrium, mg/g; c_e is the concentration of Pb(II) solution, mg/g; K_F is Freundlich constant, which is related to the adsorption capacity; and b_F is a heterogeneous factor, which is related to the adsorption strength.

3. Results and Discussion

3.1. FTIR Characterization

Figure 2 presents the infrared spectrum of chitosan, polyvinyl alcohol and PMCTS. The broad peak in the wavelength range of 3600 cm^{-1}–3200 cm^{-1} belongs to the basic characteristic band of chitosan. PMCTS had obvious absorption peaks at 2918 cm^{-1} and 1658 cm^{-1}, which were the stretching vibration absorption peaks of C-N and C-H, respectively, indicating that glutaraldehyde reacted with chitosan. The broad peak at 1068 cm^{-1} is the absorption peak of C-O-C, indicating that chitosan reacts with polyvinyl alcohol to produce a large number of ether bonds.

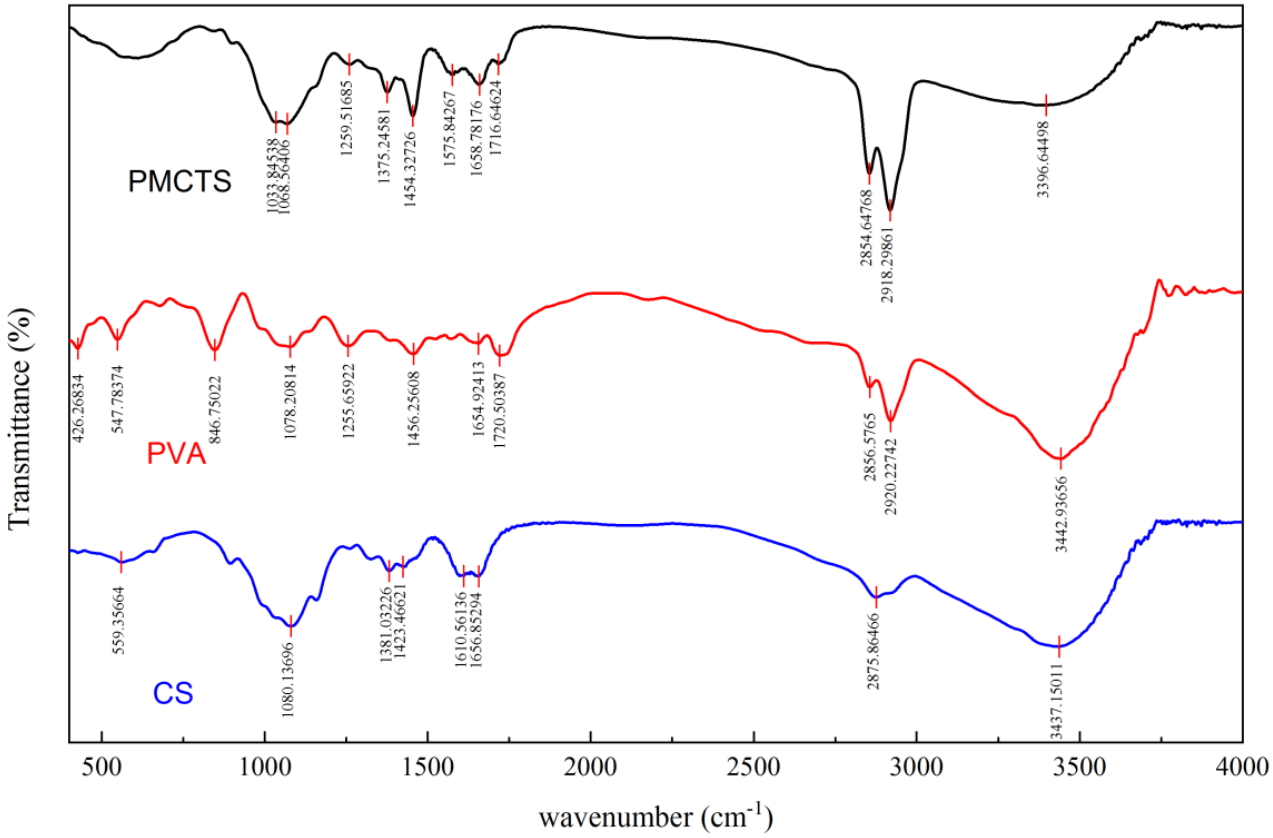


Figure 2. FTIR of chitosan, PVA and PMCTS.

3.2. XRD Measurements

It can be observed from Figure 3 that when θ is 20°, both substances have an obvious diffraction peak, which is the diffraction peak caused by the regular arrangement and crystallization of the molecular chain of chitosan [20]. The characteristic absorption peak of chitosan at 2θ = 20 ° is due to the formation of strong intermolecular hydrogen bonds and intramolecular hydrogen bonds between -OH and -NH_2 in chitosan molecules such that chitosan has good solubility. The diffraction peaks of PMCTS became sharp, which may be due to the crosslinking process affecting the degree of freedom of chitosan segments, resulting in a decrease in the regularity of the segments, in turn resulting in a decrease in its crystallinity [21]. The reason for the formation of the characteristic absorption peak of PMCTS at 2θ of 42° is that the reaction between the glutaraldehyde and -NH_2 of chitosan leads to the destruction of strong hydrogen bonds in the molecular chain of chitosan or between the molecular chains of chitosan. When chitosan is added to the solution, due to the amino protonation of the -NH_2 contained in it, chitosan becomes a charged polyelectric substance. In addition, the intramolecular and intermolecular hydrogen bonds of chitosan are vulnerable to damage, so chitosan is soluble in acid [22]. The intramolecular hydrogen bonding between the amino group of modified chitosan and the hydroxyl group of polyvinyl alcohol weakens the crystallization degree of PMCTS, indicating the amorphous properties of PMCTS. When 2θ is 30.7°, 35.7°, 43.2°, 53.1° and 62.9°, these are the (220), (331), (400), (422) and (511) crystal planes of magnetic Fe_3O_4, respectively. It was proven that Fe_3O_4 particles were successfully compounded with chitosan and PVA.

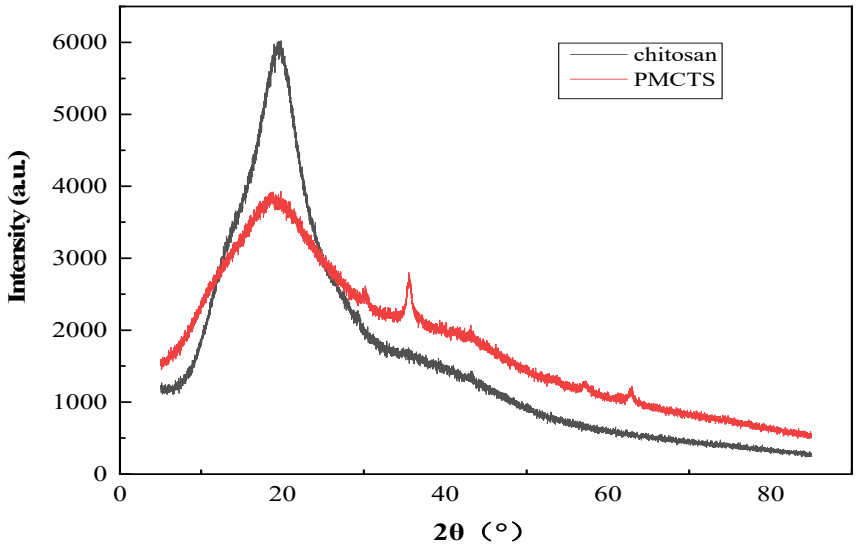


Figure 3. XRD spectrum of chitosan and PMCTS.

3.3. SEM Characterization

Figure 4 presents the microscopic surface morphology of chitosan (Figure 4(1)) and PMCTS (Figure 4(2)). From the spectrum, it can be seen that the surface of chitosan is a layered structure, with no pores and uneven dispersion; the PMCTS are relatively regular in shape and have a pore structure on the surface. This is due to the crosslinking effect of glutaraldehyde and the addition of Span-80, which causes the surfaces of the materials to increase the contact area and adsorption sites, thereby improving the adsorption capacity of the composite materials.

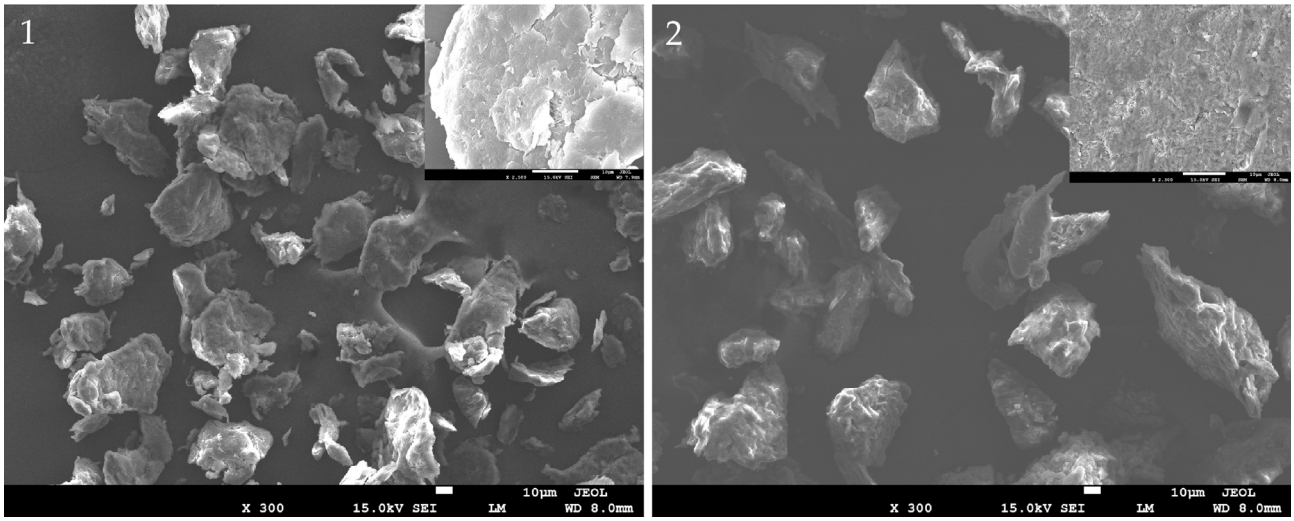


Figure 4. (**1**) SEM images of chitosan. (**2**) SEM images of PMCTS.

3.4. Magnetic Determination

Figure 5 is presents the hysteresis loop of Fe_3O_4 nanoparticles and PMCTS. It can be clearly be seen that PMCTS and Fe_3O_4 nanoparticles also have superparamagnetism, and their saturation magnetization value is 59.50 emu/g. Moreover, under the action of the magnetic field, the composite materials can be separated from the liquid in a short time, which is helpful for its separation and regeneration.

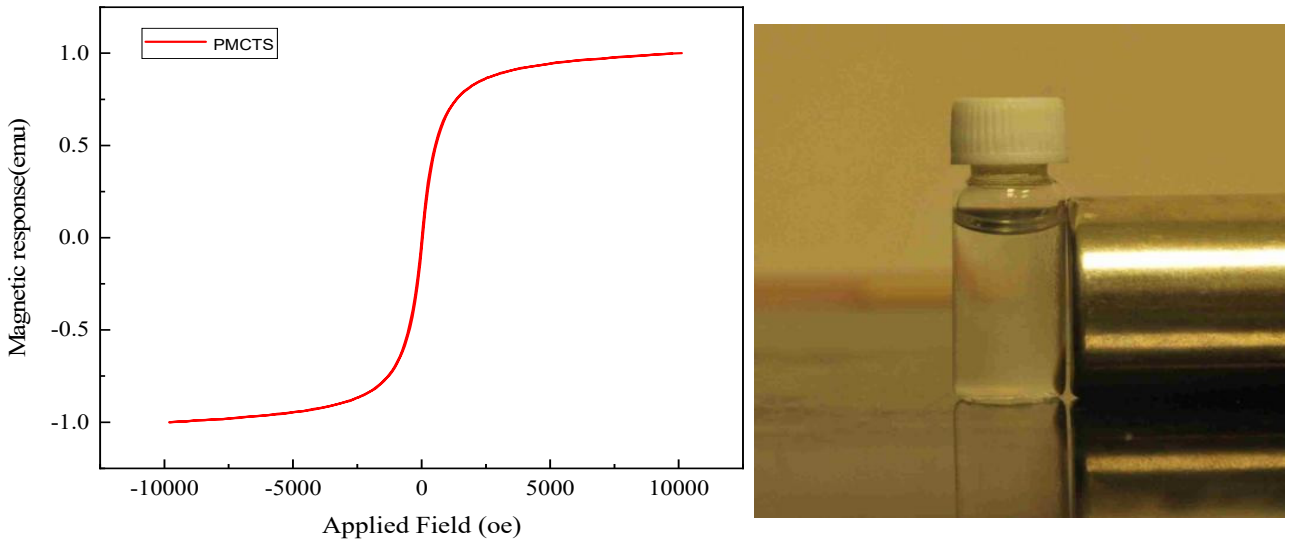


Figure 5. Magnetization curve and analysis of magnetic properties in water of PMCTS.

3.5. Analysis of Adsorption Properties of PMCTS

The single factor variable method was used to analyze the influencing factors in the adsorption process. The effects of the composite material dosage, the initial concentration of Pb(II), the adsorption time, the adsorption temperature, and the pH on the removal rate of Pb(II) were plotted, as shown in Figure 6(1)–(5).

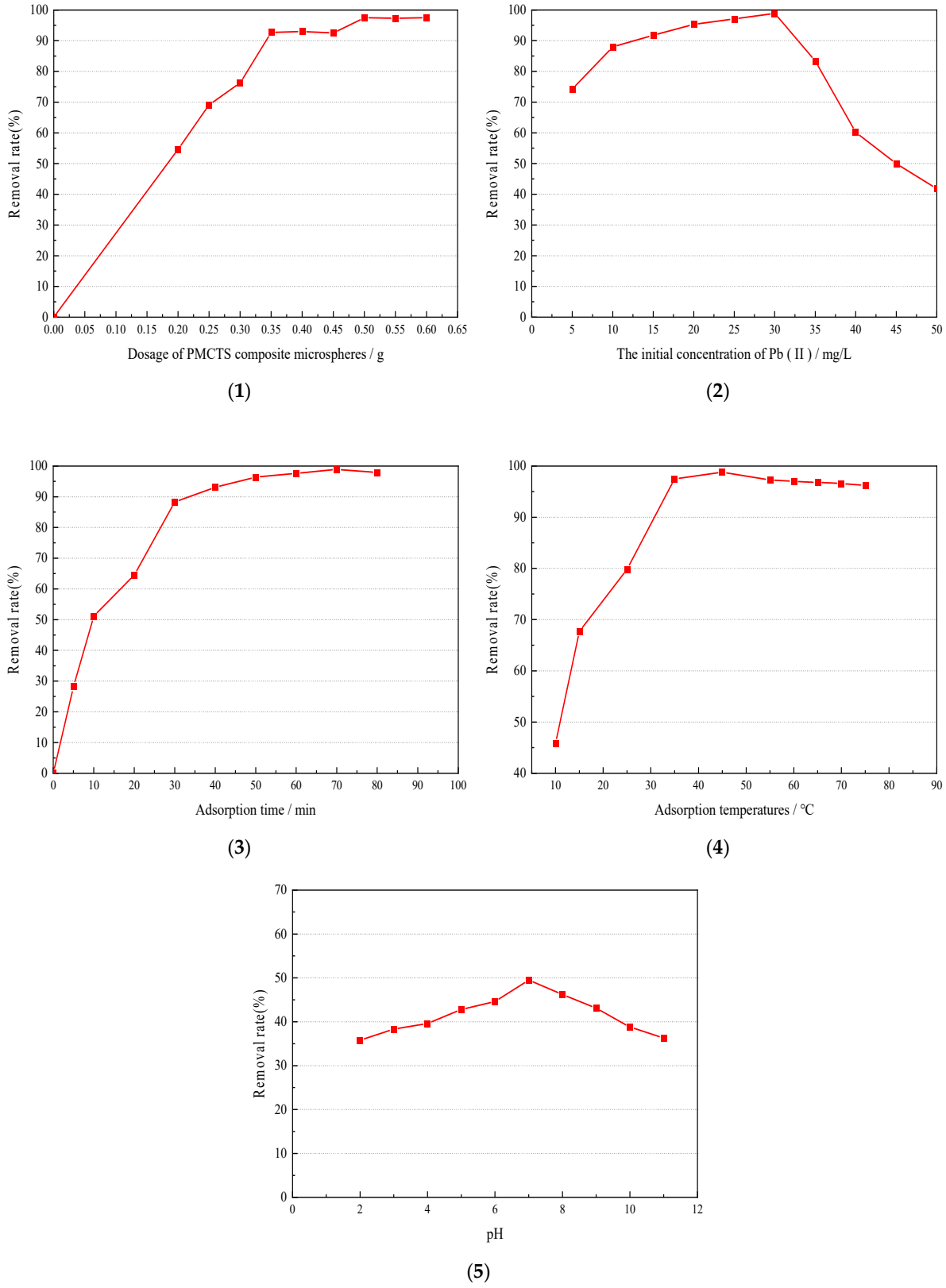


Figure 6. (**1**) Adsorption effciency curves of PMCTS for Pb(II) in solution under different dosage of PMCTS composite material conditions. (**2**) Adsorption effciency curves of PMCTS for Pb(II) in solution under different initial concentration of Pb(II) in solution conditions. (**3**) Adsorption effciency curves of PMCTS for Pb(II) in solution under different time conditions. (**4**) Adsorption effciency curves of PMCTS for Pb(II) in solution under different adsorption temperature conditions. (**5**) Adsorption effciency curves of PMCTS for Pb(II) in solution under different pH conditions.

3.5.1. Effect of PMCTS Dosage on Adsorption Effect

Figure 6(1) shows the change curve of the adsorption effect with an increase in PMCTS dosage. It can be seen that with the increase in PMCTS, the removal rate of Pb(II) is significantly increased. This is because with the increase in PMCTS in the system, the active sites that can adsorb Pb(II) increase significantly, so the adsorption capacity is enhanced, and the removal rate is obviously increasing. When the dosage is 0.5 g, the maximum value is reached, and the adsorption system reaches equilibrium.

3.5.2. Effect of Initial Concentration on the Adsorption of PMCTS

The curve of Figure 6(2) shows the change in Pb(II) removal rate with an increase in Pb(II) initial concentration. According to the observation curve, the removal rate of Pb(II) first increased and then decreased rapidly with the increase in the initial concentration of Pb(II). This is because when the amount of PMCTS in the system is constant, the number of active sites in the solution is basically constant. When the initial concentration is lower than 30 mg/L, there is a greater chance of contact between the active site and Pb(II); hence, there is a greater the removal rate. However, when the initial concentration exceeds 30 mg/L, the removal rate basically does not change. This is because the concentration of Pb(II) in the system is too high, exceeding the adsorption capacity of the material and resulting in a decrease in the removal rate.

3.5.3. Effect of Adsorption Time on Adsorption Effect

It can be seen from Figure 6(3) that PMCTS have an extremely fast adsorption capacity for Pb(II). Before 70 min, the removal rate increased rapidly with the increase in time, reaching 88.3% within 30 min. However, after the removal rate reached 98.9% at 70 min, the removal slowly decreased. This may be due to the fact that adsorption–desorption is a dynamic equilibrium process, and some Pb(II) will be re-released after reaching equilibrium.

3.5.4. Effect of Adsorption Temperature on Adsorption Effect

It can be seen from Figure 6(4) that temperature has a significant effect on the adsorption effect of PMCTS. In the range of 10–45 °C, with the increase in temperature, the contact between Pb(II) and the adsorption sites increased due to the accelerated molecular movement in the system, and the removal rate increased significantly. When the temperature increased to 55 °C, the removal rate of Pb(II) by PMCTS did not change significantly, indicating that PMCTS were a relatively stable adsorption material.

3.5.5. Effect of Initial pH Value on the Adsorption Performance of PMCTS

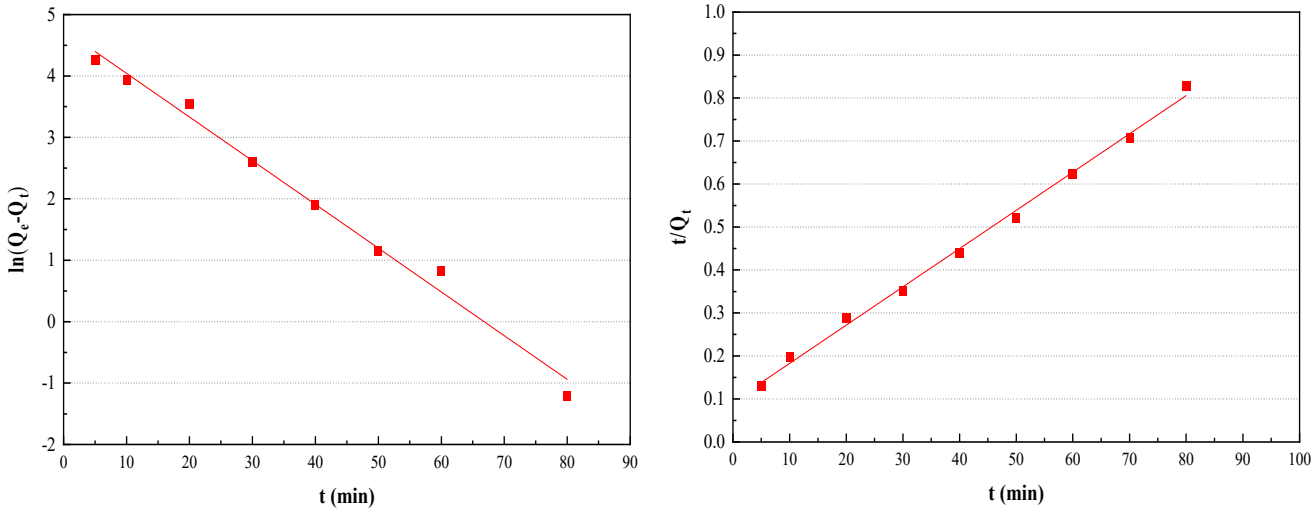
The initial pH value of the solution in the adsorption test is one of the important factors affecting the surface charge of the adsorbent, the activity of the functional group of the adsorbent, and the degree of ionization of the metal ions. The adsorption of heavy metal ions by PMCTS is mainly based on chemical complexation, mainly through the chelation of the molecular chain neutral group -NH_2 with Pb(II). Because the N atom has a lone pair of electrons, it can enter the empty orbit of Pb(II) to form a coordination bond and bind to it. The adsorption efficiency curve of PMCTS to Pb(II) in solution under different pH conditions is shown in Figure 6(5). Under the condition of pH = 7, the adsorption rate of PMCTS to Pb(II) in solution reaches its peak. Under the alkaline condition of pH < 7, the adsorption rate of CS/PVA materials to Pb(II) in solution decreased with the increase in pH value, which was due to the presence of OH^- ions in the solution, which easily react with Pb(II) in the solution to produce precipitation.

3.5.6. Recovery of PMCTS

The adsorption experiment was carried out according to the initial concentration of Pb(II) 50 mg/L. The temperature of the water bath was 45 °C, the pH was 7, and the adsorption time was 70 min. After magnetic separation, 0.916 g of composite materials was recovered, so the recovery rate was 91.6%. The experimental results show that the PMCTS have good magnetic response performance, simple separation and recovery operation, and a high recovery rate.

3.6. Adsorption Mechanisms

In this paper, the fitting of the adsorption kinetic equation is obtained according to the pseudo-first-order kinetic equation and the pseudo-second-order kinetic equation. The fitting line is shown in Figure 7, and the model parameters are shown in Table 1. By comparing the fitting results, it is found that the R^2 of the pseudo-second-order adsorption kinetic equation is significantly larger than that of the pseudo-first-order adsorption kinetic equation, and the theoretical adsorption capacity is closer to the experimental adsorption capacity. Therefore, the pseudo-second-order kinetic model is more suitable for explaining the adsorption process of Pb(II) by PMCTS.



(**1**) (**2**)

Figure 7. (**1**) Fitting lines of the pseudo-first-order kinetic equation of PMCTS for adsorption of Pb(II) in solution. (**2**) Fitting lines of the pseudo-second-order kinetic equation of PMCTS for adsorption of Pb(II) in solution.

Table 1. Pseudo-first-order kinetic equation and the pseudo-second-order kinetic equation correlation coefficients (R^2) for adsorption of Pb(II) in solution.

Pseudo-First-Order Kinetic Equation			Pseudo-Second-Order Kinetic Equation		
K_1 (min^{-1})	Q_e (mg/g)	R^2	K_2 ((mg/g)/min^{-1})	Q_e (mg/g)	R^2
0.0712	116.23	0.989	4.357×10^{-4}	112.36	0.9964

It can be seen from Figure 8 and Table 2 that the R^2 of the Langmuir adsorption isotherm is significantly greater than the R^2 of the Freundlich adsorption isotherm. Therefore, the adsorption process of Pb(II) by PMCTS material is more suitable for the Langmuir isotherm adsorption model. The adsorption process is closer to the monolayer adsorption theory.

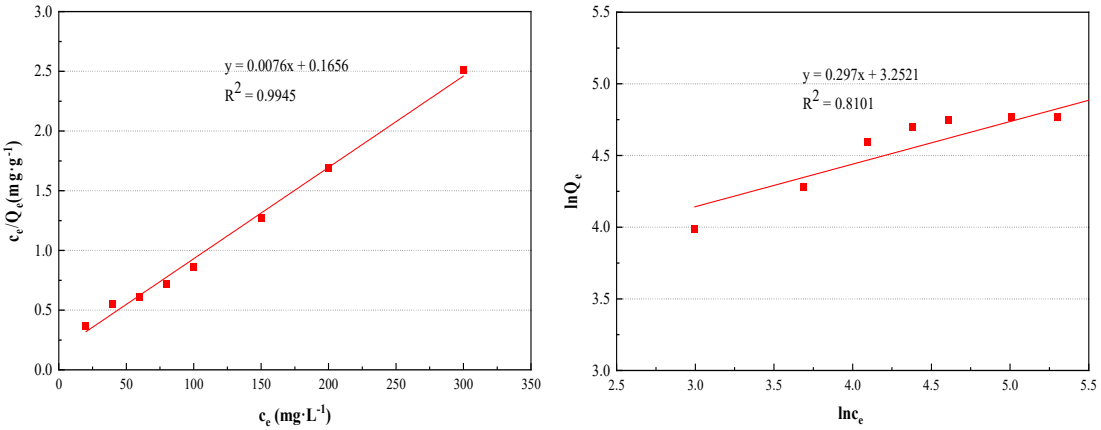


Figure 8. (**1**) Fitting curves of Langmuir adsorption isotherm of PMCTS for adsorption of Pb(II) in solution. (**2**) Fitting curves of Freundlich adsorption isotherm of PMCTS for adsorption of Pb(II) in solution.

Table 2. Isothermal adsorption model parameters of PMCTS for Pb(II) in solution.

Langmuir Adsorption Isotherm			Freundlich Adsorption Isotherm		
b (L/mg)	Q (mg/g)	R^2	K_F	b_F	R^2
0.04589	131.58	0.9945	24.85	3.367	0.8108

4. Conclusions

PMCTS were successfully prepared by inverse suspension polymerization using CS, PVA and Fe_3O_4 as the main raw materials. The chemical groups, morphological structure and magnetic properties of the composite materials were characterized. The materials were used for the adsorption of Pb(II) in water. The following conclusions were drawn: (1) PVA, Fe_3O_4 and CS were successfully copolymerized by glutaraldehyde to obtain PMCTS. PMCTS are spherical particles with a microporous structure and relatively uniform dispersion on the surface. The specific surface area is large, which is beneficial to increase the adsorption site of Pb(II). (2) PMCTS were used to adsorb and remove Pb(II) in water, showing a good adsorption effect. When the initial concentration of Pb(II) was 30 mg/L, the dosage of PMCTS was 0.5 g, the adsorption time was 70 min, pH = 7, and the temperature of the water bath was 45 °C, the maximum removal rate could reach 98.9%. (3) The recovery rate of PMCTS can exceed 91%, which proves that it has a good magnetic separation effect and a high recovery rate.

Author Contributions: X.L.: Writing—review & editing, Writing—original draft, Visualization, Methodology, Formal analysis, Data curation. W.L.: Visualization, Validation, Supervision. Y.L.: Validation, Supervision, Investigation, Conceptualization. All authors have read and agreed to the published version of the manuscript.

Funding: This work was funded by Science Research Project of Hebei Education Department (ZC2026248) and Hebei Province Chengde Center for Technological Innovation in Clean Energy and Ecological Protection.

Institutional Review Board Statement: Not applicable.

Informed Consent Statement: Not applicable.

Data Availability Statement: The original contributions presented in this study are included in the article. Further inquiries can be directed to the corresponding author.

Acknowledgments: The authors would like to thank the editors and anonymous reviewers for their insightful comments and suggestions.

Conflicts of Interest: The authors declare no conflicts of interest.

Abbreviations

The following abbreviations are used in this manuscript:

PMCTS	Composite materials
CS	Chitosan
PVA	Polyvinyl alcohol

References

1. Zamora-Ledezma, C.; Negrete-Bolagay, D.; Figueroa, F.; Zamora-Ledezma, E.; Ni, M.; Alexis, F.; Guerrero, V.H. Heavy metal water pollution: A fresh look about hazards, novel and conventional remediation methods. *Environ. Technol. Innov.* **2021**, *22*, 101504. [CrossRef]
2. Mitra, S.; Chakraborty, A.J.; Tareq, A.M.; Bin Emran, T.; Nainu, F.; Khusro, A.; Idris, A.M.; Khandaker, M.U.; Osman, H.; Alhumaydhi, F.A.; et al. Impact of heavy metals on the environment and human health: Novel therapeutic insights to counter the toxicity. *J. King Saud Univ.—Sci.* **2022**, *34*, 101865. [CrossRef]
3. Xue, X.; Han, Y.; Wu, X.; Wang, H.; Wang, S.; Zheng, J.; Ran, R.; Zhang, C. Review: Phytate modification serves as a novel adsorption strategy for the removal of heavy metal pollution in aqueous environments. *J. Environ. Chem. Eng.* **2023**, *11*, 111440. [CrossRef]
4. Khajavian, M.; Kaviani, S.; Piyanzina, I.; Tayurskii, D.A.; Nedopekin, O.V. Chitosan-based adsorptive membrane modified by carboxymethyl cellulose for heavy metal ion adsorption: Experimental and density functional theory investigations. *Int. J. Biol. Macromol.* **2024**, *257*, 128706. [CrossRef] [PubMed]
5. Jiang, W.; Yang, Y.; Miao, S.; Wan, D. Fabrication of a novel chitosan/polyaspartic acid composite: A pH-tunable sorbent for efficient adsorption of heavy metal ions and dyes from water. *J. Water Process Eng.* **2023**, *56*, 104554. [CrossRef]
6. Keshvardoostchokami, M.; Majidi, M.; Zamani, A.; Liu, B. A review on the use of chitosan and chitosan derivatives as the bio-adsorbents for the water treatment: Removal of nitrogen-containing pollutants. *Carbohydr. Polym.* **2021**, *273*, 118625. [CrossRef]
7. Zhao, G.; Wang, X.; Chen, Q.; Cheng, J. Efficacy of phosphorus loaded oyster shell in heavy metal removal: A combined study on adsorption behavior, structure characterization and comparative mechanism. *Environ. Technol. Innov.* **2024**, *33*, 103484. [CrossRef]
8. Patel, P.K.; Pandey, L.M.; Uppaluri, R.V. Highly effective removal of multi-heavy metals from simulated industrial effluent through an adsorption process employing carboxymethyl-chitosan composites. *Environ. Res.* **2024**, *240*, 117502. [CrossRef]
9. Hassan, S.S.; El-Aziz, M.A.; Fayez, A.E.-S.; Kamel, A.H.; Youssef, A. Synthesis and characterization of bio-nanocomposite based on chitosan and $CaCO_3$ nanoparticles for heavy metals removal. *Int. J. Biol. Macromol.* **2024**, *255*, 128007. [CrossRef]
10. Ghiorghita, C.-A.; Borchert, K.B.; Vasiliu, A.-L.; Zaharia, M.-M.; Schwarz, D.; Mihai, M. Porous thiourea-grafted-chitosan hydrogels: Synthesis and sorption of toxic metal ions from contaminated waters. *Colloids Surf. A Physicochem. Eng. Asp.* **2020**, *607*, 125504. [CrossRef]
11. Jin, L.; Bai, R. Mechanisms of Lead Adsorption on Chitosan/PVA Hydrogel Beads. *Langmuir* **2002**, *18*, 9765–9770. [CrossRef]
12. Kumar, M.; Tripathi, B.P.; Shahi, V.K. Crosslinked chitosan/polyvinyl alcohol blend beads for removal and recovery of Cd(II) from wastewater. *J. Hazard. Mater.* **2009**, *172*, 1041–1048. [CrossRef]
13. Laus, R.; Costa, T.G.; Szpoganicz, B.; Fávere, V.T. Adsorption and desorption of Cu(II), Cd(II) and Pb(II) ions using chitosan crosslinked with epichlorohydrin-triphosphate as the adsorbent. *J. Hazard. Mater.* **2010**, *183*, 233–241. [CrossRef] [PubMed]
14. Liu, D.; Li, Z.; Zhu, Y.; Li, Z.; Kumar, R. Recycled chitosan nanofibril as an effective Cu(II), Pb(II) and Cd(II) ionic chelating agent: Adsorption and desorption performance. *Carbohydr. Polym.* **2014**, *111*, 469–476. [CrossRef] [PubMed]
15. Kandile, N.G.; Mohamed, H.M.; Mohamed, M.I. New heterocycle modified chitosan adsorbent for metal ions (II) removal from aqueous systems. *Int. J. Biol. Macromol.* **2015**, *72*, 110–116. [CrossRef]
16. Shen, F.; Su, J.; Zhang, X.; Zhang, K.; Qi, X. Chitosan-derived carbonaceous material for highly efficient adsorption of chromium (VI) from aqueous solution. *Int. J. Biol. Macromol.* **2016**, *91*, 443–449. [CrossRef]
17. Khawar, A.; Aslam, Z.; Javed, S.; Abbas, A. Pb(II) biosorption using DAP/EDTA-modified biopolymer (Chitosan). *Chem. Eng. Commun.* **2018**, *205*, 1555–1567. [CrossRef]
18. Goudarzi, T.; Taghavi, M.; Alijani, H.; Rastegarzadeh, S. Effective remediation of mercury (II) from aqueous solutions using CS-MnFe2O4-CoS-MWCNTs: Box-Behnken design optimization and adsorption isotherm, kinetics, and thermodynamics evaluation. *Environ. Monit. Assess.* **2024**, *196*, 944. [CrossRef]

19. Wang, W.; He, H.; Wang, Z. Anionically modified chitosan-coated magnetic silica particles with enhanced adsorption for uranium removal. *J. Radioanal. Nucl. Chem.* **2025**, *334*, 6295–6303. [CrossRef]
20. Chen, C.-Y.; Yang, C.-Y.; Chen, A.-H. Biosorption of Cu(II), Zn(II), Ni(II) and Pb(II) ions by cross-linked metal-imprinted chitosans with epichlorohydrin. *J. Environ. Manag.* **2011**, *92*, 796–802. [CrossRef] [PubMed]
21. Abreu, F.O.M.d.S.; da Silva, N.A.; Sipauba, M.d.S.; Pires, T.F.M.; Bomfim, T.A.; Junior, O.A.d.C.M.; Forte, M.M.d.C. Chitosan and gum arabic nanoparticles for heavy metal adsorption. *Polim.-Cienc. E Tecnol.* **2018**, *28*, 231–238. [CrossRef]
22. Budnyak, T.; Tertykh, V.; Yanovska, E. Chitosan Immobilized on Silica Surface for Wastewater Treatment. *Mater. Sci.-Medzg.* **2014**, *20*, 177–182. [CrossRef]

Disclaimer/Publisher's Note: The statements, opinions and data contained in all publications are solely those of the individual author(s) and contributor(s) and not of MDPI and/or the editor(s). MDPI and/or the editor(s) disclaim responsibility for any injury to people or property resulting from any ideas, methods, instructions or products referred to in the content.